Investigation On The Corrosion Of Zinc Sheeting Of The Highly Insulated Cold Zinc Roofs In A Moderate Humid Region

R Zheng[1] A Janssens[2] J Carmeliet[1] W Bogaerts[3] H Hens[1]
[1] Building Physics Catholic University of Leuven Belgium
[2] Architecture and Urban Planning University of Gent Belgium
[3] Metallurgy and Materials Engineering Catholic University of Leuven Belgium

Summary: During the last decades, with increasing concerns on energy efficiency and global warming, the U-factor of building elements has been pushed towards low threshold values. The trend to lower U-factor may greatly change the hygrothermal situation of traditional cold zinc roofs. Expectedly, that change could affect the corrosion of zinc sheeting in traditional cold zinc roofs.

In order to evaluate the hygrothermal performance and durability of well-insulated zinc roofs, a long-range field test program is carried out since November 1996. A total of four cold zinc roofs with high insulation quality (U<0.25 W/m^2/K) were constructed on the campus of KU Leuven, Belgium. Commercial zinc sheeting of 0.65 mm thickness (VM-zinc titanium) was used.

Investigations were conducted on the corrosion of zinc sheeting of the zinc roofs. The results showed: (1) The underside corrosion of the zinc sheeting was severe and far more serious than the upside corrosion. (2) Pitting was the main form of corrosion of the zinc sheeting. (3) A more perfect air-vapor tight retarder and a good ventilation of the roof cavity could not guarantee an elimination or a reduction of the underside corrosion of zinc sheeting in ventilated zinc roofs.

Keywords: Metallic roofs, corrosion, thermal insulation

1 INTRODUCTION

Zinc roofing is common in Europe and may provide satisfactory service lives in urban atmospheres. It is usually considered to be maintenance-free, have a long life span, and easily adaptable to various design styles ranging from traditional to modern. The good performance of traditional zinc roofs is mainly attributed to the excellent resistance of zinc to corrosion and the favorable micro-environment surrounding the zinc sheeting.

Traditional cold zinc roofs were constructed with low insulation quality (most of them U>0.6 W/m2/K) and good ventilation. When carefully designed and installed, the condensation problem at the underside of zinc sheeting could be avoided or the condensate on underside surface of the zinc sheeting could dry out quickly. The underside corrosion of the zinc sheeting was not a serious problem. Traditional cold zinc roofs therefore performed well and served for a long time. Normally, a traditional cold zinc roof had a life span of over 30~40 years in industrial areas and of over 100 years in rural areas. In typical urban areas, a life span of 50~60 years could be expected.

Nevertheless, in the last decades, the growing concerns about global warming and energy efficiency pushed the U-factor of building elements towards low threshold values. This trend to lower U-factors may greatly affect the performance of zinc roofs due to a worse hygrothermal environment surrounding the zinc sheeting. The lower U-factors in fact may result in stronger undercooling of the zinc sheeting and in lower air temperature in the roof cavity. This will decrease the removal of water vapor from the roof cavity by ventilation, which is usually considered to be a good solution to avoid condensation at the underside of zinc sheeting. In the worse cases, the phenomenon of undercooling may be so strong that the temperature of the zinc sheeting may drop below the dew-point temperature of the surrounding air. This makes the surrounding air to become a moisture source so that the effect of ventilation shifts from drying to wetting the zinc sheeting. Therefore, cold zinc roofs with high insulation

quality may have a serious problem of corrosion at the underside of the zinc sheeting. Unfortunately, little research has been conducted on that problem.

In order to investigate the hygrothermal performance and durability of well-insulated zinc roofs, in November 1996, a long-range field test program was started in the VLIET test building of the Laboratory of Building Physics of the K.U.Leuven. This paper presents some results of this field study.

2 EXPERIMENTAL DESIGN AND EXPOSURE CONDITIONS

2.1 Experimental design

A total of four cold zinc roofs with high insulation quality (U < 0.25 W/(m²·K)) were constructed on the campus of KU Leuven, Belgium, in 1996. The dimensions of the roofs were about 1.8 by 3 m. The roof slope was 5 %. The orientation of two roofs was southwest (SW1c and SW2c), of the other two northeast (NE1c and NE2c). Of the four cold zinc roofs, NE2c and SW2c had a correctly installed air-vapor retarder, the others (NE1c and SW1c) a poorly installed air-vapor retarder. The section of the zinc roofs is shown in Fig. 1. The details are presented in table 1. In order to simulate the installation of electrical connections, a perforation of 47 mm in diameter through the gypsum board and the air-vapor retarder was made in the roofs SW1c and NE1c (hereafter referred SW1c and NE1c as air-open roofs, the other two zinc roofs without a perforation being called air-tight roofs) respectively. The perforation was located at the center of the air-open zinc roofs.

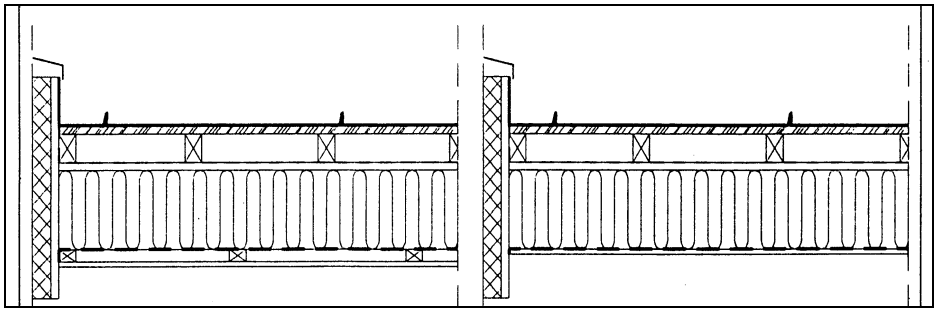

Air tight (SW2c, NE2c) Air open (SW1c, NE1c)

Figure 1. The cold zinc roofs

Table 1 The cross sections of the cold zinc roofs (from outside to inside)

Cold zinc roofs: air- tight (SW2c, NE2c)	*Cold zinc roofs: air-open (SW1c, NE1c)*
• zinc sheeting with standing seams	• zinc sheeting with standing seams
• pine boarding 3/4"	• pine boarding 3/4"
• rafters 38×58 mm with ventilated cavity	• rafters 38×58 mm with ventilated cavity
• vapor open underlay foil	• vapor open underlay foil
• mineral wool 15 cm between rafters 60×175 mm	• mineral wool 15 cm between rafters 60×175 mm
• polyethylene (0.2 mm) air-vapor retarder	• polyethylene (0.2 mm) air-vapor retarder with a perforation ∅ 47 mm
• painted gypsum board	• painted gypsum board with a perforation ∅ 47 mm

2.2 Exposure conditions

The weather data were automatically recorded every ten minutes in the weather station and transported to a computer. The main weather parameters recorded were wind speed, wind direction, solar radiation, air temperature, and relative humidity. The temperature, relative humidity, wind speed and wind direction were measured at a height of 9 m above ground level. The radiation was measured at the southwest edge of a paved roof. Both the inside and outside monthly average climatic information for the exposure experiod are presented in table 2.

Table 2 Outside and inside climatic parameters during the exposure period of 28 months.

Month	*Outside*				*Inside the house*	
	Temperature °C	*Relative humidity %*	*Solar gain (horizontal surface) W/m²*	*Wind velocity m/s*	*Temperature °C*	*Relative humidity %*
Dec-96	0.7	81	20	1.7	22.6	42
Jan-97	-0.4	83	30	1.2	22.6	43
Feb	7.3	78	48	2.9	22.5	49
Mar	8.9	81	93	1.6	21.8	56
Apr	8.6	69	164	1.6	22.3	48
May	13.7	73	208	1.6	22.6	55
Jun	16.5	74	202	1.5	23.3	57
Jul	17.7	80	195	1.0	23.4	65
Aug	21.2	76	195	1.1	25.6	58
Sep	14.7	80	139	0.9	22.6	62
Oct	10.5	81	80	1.4	22.6	51
Nov	7.8	88	33	1.7	22.4	50
Dec	6	85	20	2.4	22.5	49
Jan-98	5.3	81	27	2.6	22.5	43
Feb	6.5	80	61	1.5	22.9	42
Mar	8.3	79	80	2.1	22.9	45
Apr	9.9	81	125	1.9	22.9	47
May	15.8	73	197	1.3	22.6	43
Jun	16.8	79	197	1.4	23.4	52
Jul	16.5	82	142	1.1	23.0	60
Aug	14.7	86	126	1.2	23.2	49
Sep	15.7	86	107	1.3	22.6	63
Oct	10.5	88	47	2.0	22.5	53
Nov	4.4	88	38	1.5	22.8	40
Dec	5.5	88	19	2.1	22.2	44
Jan-99	6.4	84	30	2.4	22.8	44
Feb	3.8	87	53	1.9	23.1	43
Mar	8.2	81	97	1.9	23.0	49

2.3 Collection of zinc specimens

One large zinc specimen was taken from each zinc roof in March 1999. The dimensions of the specimens were 50 by 70 cm. Each specimen contained a standing seam. All were visually examined on the spot. The location of the collected large zinc specimens on the zinc roofs is shown in Fig. 2.

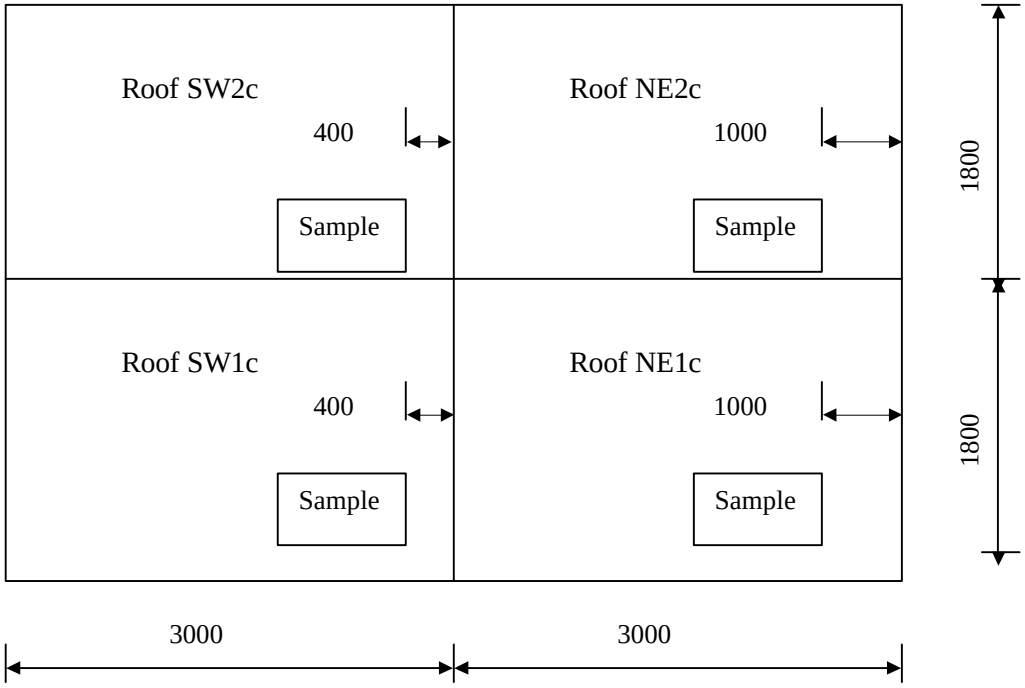

Figure 2 The location of the collected large zinc specimens in the cold zinc roofs (top view)

2.4 Cleaning method

In order to evaluate the corrosion type and the corrosion rate of the sheeting, some small samples were cut from the large specimens. These small samples were cleaned chemically as proposed by ASTM Standard G1-90: Practice for Preparing, Cleaning, and Evaluating Corrosion Test Specimens (ASTM Designation: G 1-90, 1994). The samples were first immersed in warm (70 °C) ammonium chloride solution (10 %) for 5 minutes, rinsed in reagent water, and scrubbed with a light brush. Then, an ultrasonic cleaning machine (BRANSON-1200) was used to remove the remaining corrosion products from the deep pits. The above procedure was repeated two times. Removal was confirmed by examination with a low power microscope (5 to 50 ×). After the final treatment, the zinc samples were thoroughly rinsed and immediately dried.

3 CORROSION TYPE OF ZINC SHEETING

3.1 General description of distribution of corrosion products

As shown in Fig. 3, the distribution of white corrosion products was not uniform at the underside of the zinc sheeting. It is also noted that there was no much apparent difference in corrosion between the air-open cold zinc roofs (SW1c and NE1c) and the air-tight cold zinc roofs (SW2c and NE2c). Generally, in light of the distribution of the corrosion products, there existed two typical regions on the underside of the large specimens. One region was heavily covered with white corrosion products (here labeled type I), the other was covered by a thin white film of corrosion products (here labeled type II). The directional characteristic of rolled zinc sheeting can clearly be seen on the areas with a thin white film of corrosion products.

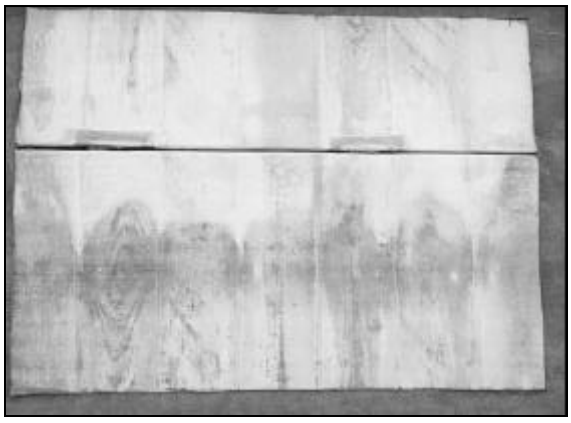

Roof NE1c

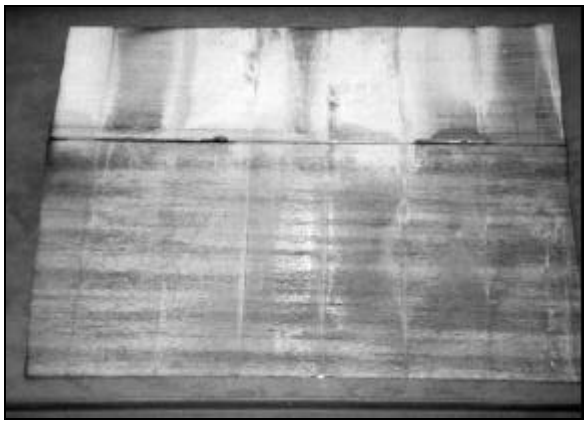

Roof SW1c

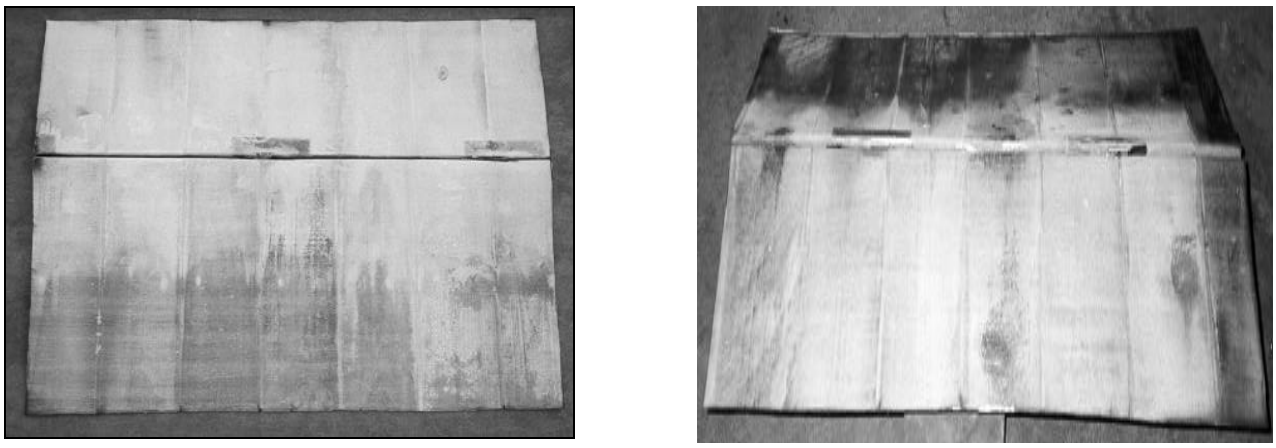

Roof NE2c Roof SW2c

Figure 3 Large zinc specimens taken from the cold zinc roofs (50´70 cm)

Figure 4 illustrates a wood scar on the wood deck in NE1c and the appearance of the corrosion product on the zinc surface corresponding to the scar. We believe that the underside surface of the zinc sheeting somewhat touched the wood scar due to the sign of the scar on the zinc surface. Examining it carefully, it is found that the center area of the wood scar was a little higher than the edge area. The height gradually reduced along the annual ring of the scar from the center to the edge. So, if the zinc sheeting contacted the wood scar, the most possible contacting place was the center area. Making a comparison between them, it is noted that the corrosion of the zinc sheeting corresponding to the center area of the wood scar was lighter than that corresponding to the edge area of the wood scar. This may partly demonstrate the influence of the contact situation between the zinc sheeting and the wood deck on the appearance of corrosion products on the zinc surfaces. For our cases, we may say that the corrosion pattern on the zinc sheeting contacting the wood deck or having much small gaps between the zinc sheeting and the wood deck took the type II, while that in the no-contact areas took the type I.

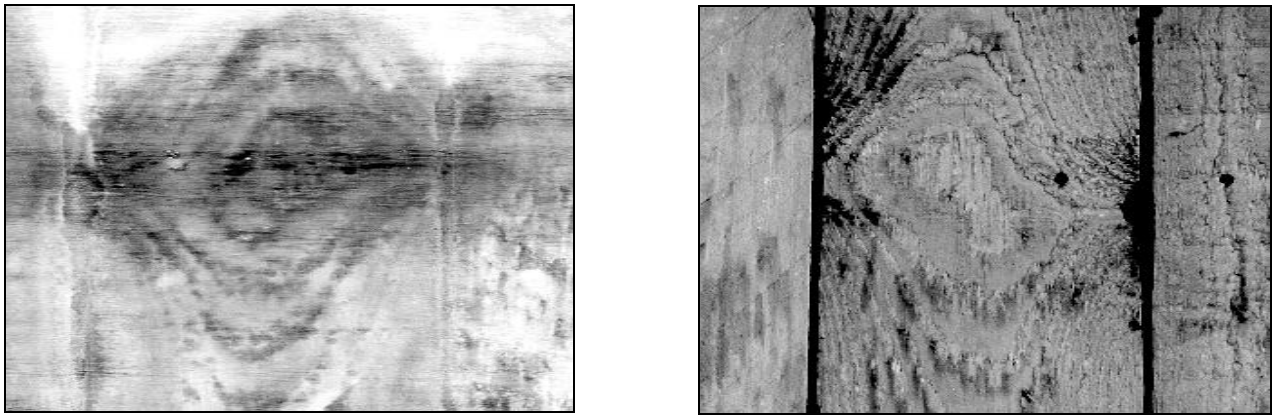

Figure 5 Area of the zinc sheeting contacting a wood scar (left) and the corresponding wood scar in the wood deck (light)

3.2 Type of corrosion

The types of corrosion that are commonly found to occur on zinc sheeting can be divided into four groups, namely general corrosion, pitting corrosion, galvanic corrosion, and intergranular corrosion. Of the corrosion types, general corrosion is most common.

Figure 6 shows the typical appearances of the underside of the zinc sheeting in the no-contacting areas after removal of the corrosion products. Clearly, a lot of big pits developed on the surface. The distribution of the pits was roughly uniform, but the dimension had some variation. Figure 7 illustrates the typical appearance of the underside of the zinc sheeting in the contacting areas after removal of the corrosion products. The zinc surface developed some dull appearance and the pits were very small. The distribution of these small pits was quite uniform. The corrosion at the no-contacting areas was much more serious than that at the contacting areas. The pits in both the no-contacting areas and contacting areas generally took a circular shape.

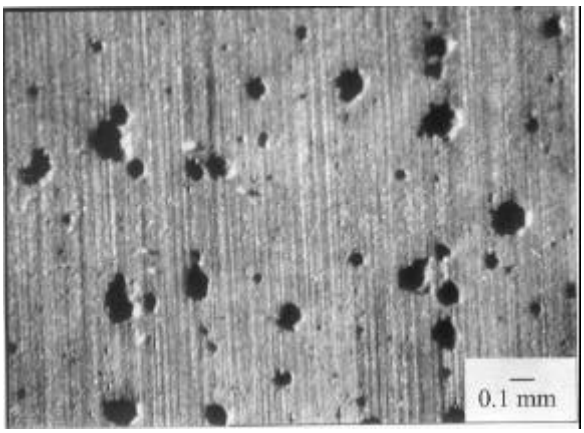

Figure 6 The typical appearance of the underside of the zinc sheeting in the area not contacting the wood deck after removal of the corrosion products

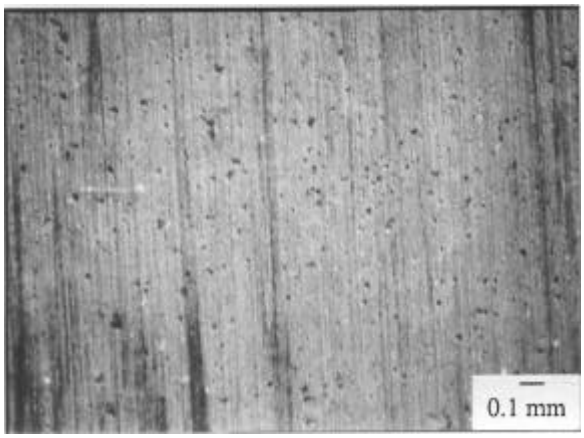

Figure 7 The typical appearance of the underside of the zinc sheeting in the area contacting the wood deck after removal of the corrosion products

For the upside of the zinc sheeting, the typical appearance after removal of the corrosion products is shown in Fig. 8. It is obvious that numerous small pits developed over there. The distribution of the pits is quite uniform from a macroscopic point of view. The pits seem shallow and many of their depths might be smaller than their diameters.

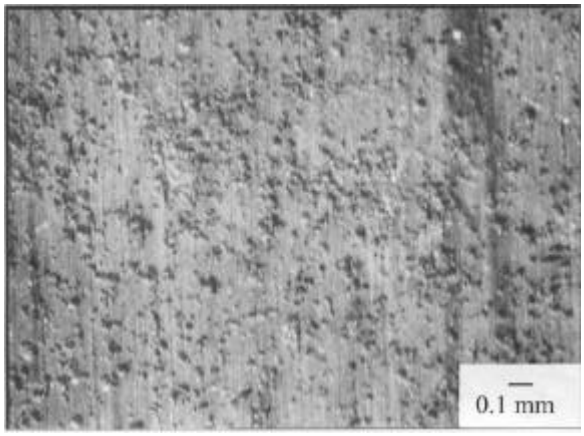

Figure 8 The typical appearance of the upside of the zinc sheeting after removal of the corrosion products

4 CORROSION RATE OF ZINC SHEETING

4.1 Method of evaluation

It is well know that pitting corrosion can be more serious than general dissolution attack. The growing rate of pit depth is dependent on both the environmental and the metallurgical conditions. It is very important to be able to determine the extent of pitting corrosion, either in a service application where it is necessary to predict the service life of zinc roofs, or in laboratory test programs that are used to select the best structures for zinc roofs.

In evaluating pitting corrosion, both the average corrosion rate based on mass loss and the average pit depths cannot readily be used. The corrosion estimation based on mass loss can seriously underestimate the corrosion penetration caused by pitting. For the corrosion estimation based on the average pit depth, there are also some problems. First, many smaller pits become too indistinguishable to be measured due to stopping growth very soon after initiated, and second, the deeper pits are of most practical importance.

For metallic roofs, the deepest pits will initiate leakage if they continue to propagate. Therefore, it is not the overall corrosion rate or the number of pits that are of interest, but the deepest pits since they cause the failure of the roof. Of the available evaluating methods, the extreme value statistical theory has been proven to be a powerful tool to analyze maximum pit depth data. This theory can be used to estimate the maximum pit depth of a large area of material on the basis of the examination of a small portion of it. Thus, we used the statistical theory of extreme value to evaluate the corrosion rate of the zinc sheeting.

4.2 Collection of maximum pit depths

As shown above, the corrosion situations in the contact areas and no-contact areas were quite different. Considering the quite light extent of pitting corrosion in the contact areas, we only evaluated the extent of pitting corrosion in the no-contact areas.

A total of ten small samples (5×5 cm) were collected from each area under concern on the large zinc specimens. The small samples were cleaned chemically using the method described previously. Five possible deepest pits on each sample were located by examination under a low-power microscope (5 to 50 ×) and were circled with a pencil. Then, the circled pits were measured using a powerful microscope "Quick Vision" (200 to 1000 ×). A pit was centered under the objective lens at low magnification, which was increased until the pit area, including the lips, filled most of the field of vision. The microscope was first focused on the uncorroded surface at the lips of the pit and then on the lowest part at the bottom of the pit. The difference between the initial and the final reading was counted as the pit depth. On a single pit, the measurement was repeated three times and the largest value was selected as depth of the pit. Of the depths of the possible five deepest pits on each sample, the largest one was considered to be the maximum pit depth of that sample. The measured maximum pit depths for each zinc roof based on the ten small samples are given in table 3.

Table 3 The measured maximum pit depth of each zinc roof based on the ten small samples

Roof	*SW1c*	*NE1c*	*SW2c*	*NE2c*
Maximum depth (μm)	167	180	273	228

4.3 Type of distribution of the maximum pit depths

Table 4 presents the results of a statistics analysis on the measured maximum pit depths. Since the maximum depths at the upside of the zinc sheeting were too small to be located and measured, they are not considered in the analysis. As shown in Table 4, all Fs are far less than 0.01. This shows that the linear regression relationships between the reduced variates and the maximum pit depths are highly significant. This can be taken as a proof that the maximum pit depths are sampled from parent populations of the exponential type and that the infinite population of maximum pit depths follow the Gumbel distribution.

Table 4 Equations of linear regression between the reduced variates and the maximum pit depths in the cold zinc roofs

Roofs	Equations of linear regression	R square	F (significance of F-test)
SW1c_nca	y = 0.031943*x - 3.09361	0.969	2.63E - 07
NE1c_nca	y = 0.059071*x - 8.33586	0.954	1.21E - 06
SW2c_nca	y = 0.023750*x - 4.19073	0.962	5.62E - 07
NE2c_nca	y = 0.042821*x - 7.96814	0.921	1.09E - 05

Note: "nca" — no-contact areas.

4.4 Estimation of the maximum pit depth on the zinc roofs

It is interesting to know how many maximum depth pits deeper than a specific value may exist in a zinc roof. Since the number of the maximum depth pits is area dependent, both the contact area and the no-contact area should be known for this analysis. Nevertheless, there is some difficulty of obtaining the exact areas of the contact surface and no-contact surface for the entire zinc roofs in practice. On the basis of the appearance of the large zinc specimens, we assumed that the ratio of the contact area to the no-contact area was 0.4:0.6, without regard to the very little pits in the contact areas. Thus, the cumulative probability of the maximum pit depths can be expressed as

$$1-\frac{m}{N_C}=0.6\times\exp\left(-e^{-\frac{x_C-u_{nca}}{\alpha_{nca}}}\right)+0.4 \qquad (1)$$

Where:

m — the number of maximum depth pits deeper than a specific value

N_c — the total number of small samples for each cold zinc roof.

α_{nca} and u_{nca} — The scale value and mode value of the distribution of the maximum pit depths in the no-contact areas

x_c — the specific maximum depth, μm.

Rearranging the equation (1), the specific value x_c that there are m maximum depth pits deeper than x_c can be expressed as

$$x_C = u_{nca} - \alpha_{nca} \ln\left(\ln\left(\frac{0.6N_C}{0.6N_{C-m}}\right)\right) \quad (2)$$

Table 5 summarizes the values of x_c obtained from equation (2) for m = 1, 10, 50, and 100. It is evident that, for all cases in question, the values of the pit depths in SW2c and NE2c (the two roofs with a correctly installed air-vapor retarder) were much larger than those in SW1c and NE1c (the two roofs with a poorly installed air-vapor retarder). This means that the maximum pit depths in SW2c and NE2c were much deeper than those in SW1c and NE1c. For the comparatively deep maximum depth pits (i.e., m = 1 and 10), the maximum pit depths in SW1c and SW2c were deeper than those in NE1c and NE2c, respectively.

Table 5 The values of x_c in the cold zinc roofs (unit: mm) when m = 1, 10, 50, and 100.

Number of pits	SW1c	NE1c	SW2c	NE2c
1 pit	321	262	479	353
10 pits	249	223	382	299
50 pits	198	196	313	262
100 pits	176	184	283	245

4.5 Estimation of the failure probability of the zinc roofs

Perforation of zinc sheeting is one of the most important factors in determining the service life of zinc roofs. The first perforation, whose time and location is a matter of probability, is a useful indicator to reveal the situation of the zinc sheeting. It is very important to know the probability of failure. In the following analysis, we consider the zinc sheeting to fail once there exists a maximum depth pit deeper than the thickness of the sheeting.

The failure probability of the no-contact areas of the individual zinc roof P_{nca} may be written as

$$P_{nca} = 1 - \exp\left(-e^{-\frac{x_t - u_{nca} - \alpha_{nca}\ln 1296}{\alpha_{nca}}}\right) \quad (3)$$

where:

x_t — The thickness of zinc sheeting in microns, 650 μm.

Considering the very small pits in the contact areas, we may assume its failure probability P_{ca} to be zero. The events P_{nca} and P_{ca} are independent. Thus, the failure probability of a cold zinc roof is given by

$$P_C = 1 - \exp\left(-e^{-\frac{x_t - u_{nca} - \alpha_{nca}\ln 1296}{\alpha_{nca}}}\right) \quad (4)$$

Table 6 summarizes the failure probability of the cold zinc roofs. As seen in table 6, the failure probability in SW2c and NE2c is obviously higher than that in SW1c and NE1c, respectively. It is also noted that the probability of failure in SW1c and SW2c is clearly higher than that in NE1c and NE2c, respectively.

Table 6 Failure probability of the zinc roofs

roof	*SW1c*	*NE1c*	*SW2c*	*NE2c*
Failure probability	2.77E-5	1.14E-10	1.70E-2	3.04E-6

5 DISCUSSION

It was expected that no severe corrosion was found on the upside of the zinc sheeting in the zinc roofs because a specific protection layer developed there as time progresses. This layer contains zinc hydroxide and basic zinc salts and is called patina. It is this layer that prevents the upside of the zinc sheeting from being seriously attacked. Although numerous very little pits developed on the upside surface, they normally are not a big problem. Pitting corrosion in atmospheric environments has seldom been reported as the main cause of failure of zinc sheeting. Pitting corrosion is normally induced in clean rural environments. While the depth of the pits increases with time, the ratio of pit depth to surface-average corrosion penetration decreases (Zhang, 1996). In an ASTM atmospheric exposure program, pits were observed on high-grade zinc and on a 1% Cu-

zinc alloy after two years of exposure in four different environments (Showak and Dunbar, 1982; Viart, 1984). In general, the upside pitting corrosion of the zinc sheeting may have little impact on the service life of the zinc roofs in question.

Normally, contact between zinc and hygroscopic materials, especially in moist conditions, may result in more severe corrosion. Obviously, as shown, it was found that the underside corrosion of the zinc sheeting was more severe in the no-contact areas than in the contact areas. This may be attributed to the strong undercooling of the sheeting.

The measured undercooling of the sheeting could be so severe that its temperature fell below the dew-point of the outdoor air for quite a long time. Due to the seams (about 5 mm) among laths in the wood deck, the ventilated air in the roof cavity might bypass the laths and reach the underside of the zinc sheeting. So, condensation induced by ventilation could occur in those non-contact areas during severe undercooling periods. That caused the underside corrosion of the sheeting.

For the areas contacting the wood deck or the areas with much small gaps between the sheeting and the wood, however, less condensation might be expected because of the difficulty of ventilated air reaching those spots and because of the hygroscopic inertia of the wood. The wood deck absorbs the little condensation if any. In these areas, the corrosion rate of the zinc sheeting mainly depends upon the moisture content in the wood deck. Its threshold value to induce zinc corrosion is about 20 % by weight (Building Research Establishment, 1986). Therefore, if the moisture content in a wood is continuously kept below that critical level, zinc does not suffer severe corrosion even contacting the wood. As the moisture contents in the wood deck during the last three years of measurement generally remained lower than 20 %, it is reasonable that less corrosion at the underside of the zinc sheeting in the wood-contact areas occurred in comparison with the no-contact areas.

It has been widely accepted that high inside air exfiltration and poor ventilation of roof cavity are the main factors resulting in severe underside corrosion of zinc sheeting in cold roofs. The precautions against the underside corrosion of the sheeting mainly focus on these two aspects. Dunbar and Showak (1982) proposed two basic measures to eliminate or reduce this type of corrosion: 1. Installing a good vapor barrier underlay material under the zinc sheeting to minimize the amount of water vapor that can permeate and condense against its underside. 2. Providing some airflow between the zinc sheeting and the underlay to rapidly dry any moisture that does condense. In order to increase the ventilation in roof cavity, Zaher (1995) recommended that zinc roof slopes should be more than 1 in 12, otherwise, additional venting is needed to assist the drying of the underside of zinc sheeting.

The ventilation in the roof cavity of the cold zinc roofs in the test building has been investigated by Janssens (1997). It was found that the relation between the ventilation rate (G, $m^3/m/h$) and the wind speed (v, m/s) was "G = 27.8 v". This result showed that wind could induce a good ventilation rate in the cavity of the cold zinc roofs on the test building. Obviously, that good ventilation could not eliminate or lessen underside corrosion of the sheeting in these highly insulated cold zinc roofs. It is found unexpectedly that the underside corrosion of the zinc sheeting in SW2c and NE2c (air-tight zinc roofs) was more severe than that in SW1c and NE1c (air-open zinc roofs). Apparently, the low air exfiltration could not eliminate or even reduce underside corrosion of the sheeting in these highly insulated cold zinc roofs either.

A possible reason for the unexpected results is the strong undercooling of the sheeting. Zheng et al (1999) made an investigation on the hygrothermal behavior of the zinc roofs. The results showed that the severe undercooling of the sheeting could make the surrounding air to become a moisture source so that the effect of ventilation was changed from drying to wetting the underside of the sheeting. Under that situation, more air exfiltration combined with good ventilation of the cavity might increase the thickness of water layer at the underside of the sheeting. It is well known that the thickness of water film on zinc surface is one of the most important factors affecting the corrosion rate of zinc in atmosphere. Thicker water film decreases the diffusion rate of oxygen. In this situation, the thicker the water layer, the lower the corrosion rate was.

As shown, the traditional precautions (low air exfiltration and good ventilation in cavity) seem not to work effectively in cold zinc roofs with high insulation quality. New techniques and roofing systems should be developed, if we like to guarantee a significant reduction of underside corrosion in zinc roofs with high insulation quality.

6 CONCLUSIONS

A field investigation was performed to evaluate the corrosion type and corrosion rate of the zinc sheeting in the highly insulated cold zinc roofs in a moderate humid region. The following main conclusions were drawn:

1. Numerous very little pits developed on the upside of the zinc sheeting. The distribution of the pits was quite uniform. The upside of the zinc sheeting corroded very little.
2. At the underside of the zinc sheeting, pitting corrosion was the prevailing corrosion type.
3. There existed two different forms of underside corrosion of the zinc sheeting. In the areas where contacted the wood deck, its surface developed some extent of dull appearance and only somewhat pitting corrosion occurred; while in the areas not contacting the wood deck, numerous large and deep pits developed.
4. The low air exfiltration and the good ventilation in the roof cavity could not guarantee an elimination or even reduction of the underside corrosion of the sheeting.
5. Generally speaking, the corrosion of the sheeting was very severe in the highly insulated cold zinc roofs after being exposed for only three years.

6. New techniques and roofing systems should be developed for highly insulated zinc roofs in moderate humid regions.

7 ACKNOWLEDGMENTS

The financial support from the Flemish government and the KU Leuven and the industrial support from Union Miniere are gratefully acknowledged. The authors would like to thank E. Verstraeten for the help on the sample cleaning and S.Z. Song for the help on the measurement of pit depths.

8 REFERENCES

1. ASTM Designation G1-90 1994, Standard practice for preparing, cleaning, and evaluating corrosion test specimens, Annual book of ASTM standards, Volume 03.02, Wear and Erosion; Metal Corrosion.
2. Building Research Establishment 1986, Zinc-coated steel, Building Research Establishment Digest, Digst 305, UK, January.
3. Dunbar, S. R. & Showak, W. 1982, 'Atmospheric corrosion of zinc and its alloys', in Atmospheric Corrosion, eds W. H. Ailor, John Wiley & Sons, New York, pp. 529-552.
4. Janssens, A. 1997, VLIET PROEFGEBOUW, DEEL 3: ZINKEN DAKEN, TWEEDE JAARRAPPORT, (VLIET Test Building, Part 3 : Zinc Roofs, the second year report), Laboratorium Bouwfysica, K. U. Leuven, Belgium. (in Dutch).
5. Showak, W. & Dunbar, S. R. 1982, 'Effect of one percent copper addition on atmospheric corrosion of rolled zinc after 20 year's exposure', in Atmospheric Corrosion of Metals, STP 767, pp. 135-162, ASTM.
6. Viart, G. 1984, 'Galvanised steel wire with high corrosion resistance', Wire Ind., Vol. 83, 76-78.
7. Zahner, L. W. 1995, Architectural Metals: a guide to selection, specification, and performance, John Wiley & Sons Inc..
8. Zhang, X. G. 1996, Corrosion and electrochemistry of zinc, Plenum Press, New York.
9. Zheng, R., Janssens, A. & Hens, H. 1999, 'A field study of hygrothermal performances of low slope highly insulated zinc roofs in moderate humid regions', Proc. 10th International Symposium for Building Physics, TU Dresden, Dresden, Germany, 27-29, September 1999, vol. 1, pp.251-261.